Supplementary Figures

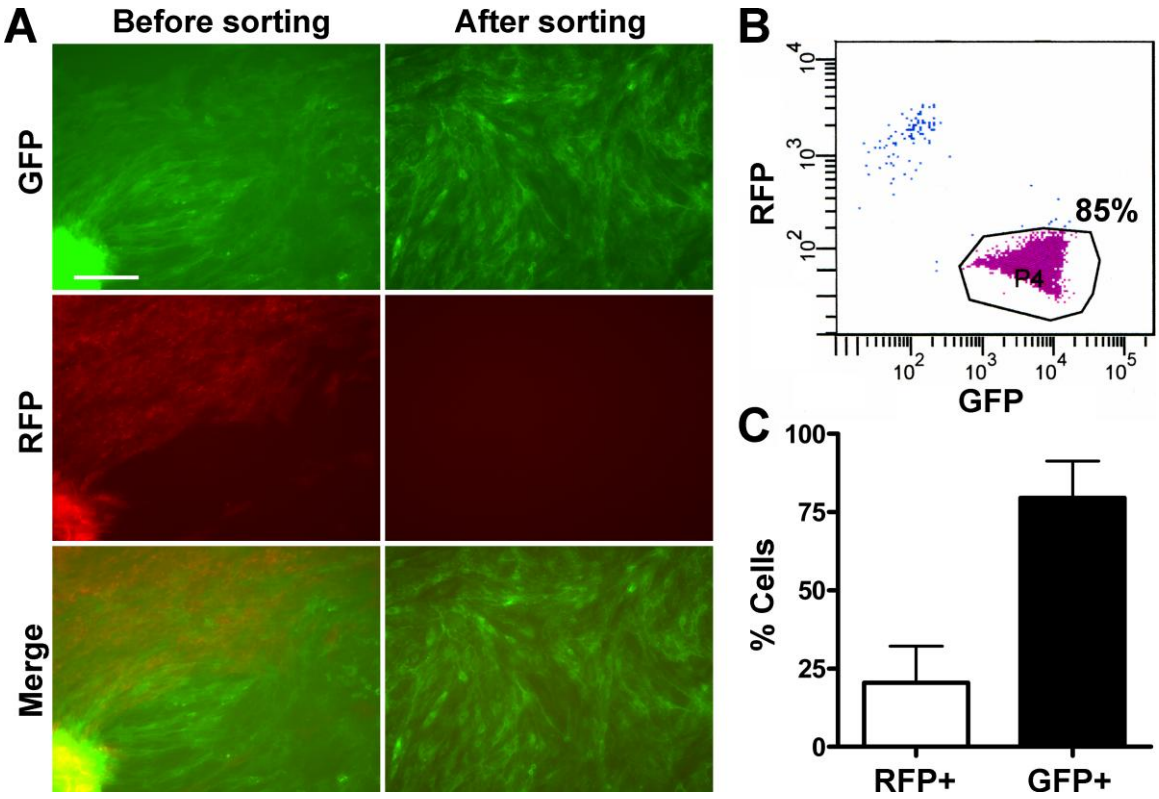

Figure S1. Isolation of genetically-defined SMCs. *mT/mG.Myh11-CreER^{T2}.Tgfbr2$^{f/f}$* mice were treated with tamoxifen for 5 d starting at 4 wk of age and the thoracic aorta was harvested at 8 wk. The adventitia and endothelium were sharply removed under magnification and the medial cells were isolated after enzymatic digestion. (***A***) Using conventional SMC isolation techniques, GFP$^+$ cells were contaminated with a minor population of RFP$^+$ cells that tended to overgrow the cultures. After sorting by flow cytometry, a highly purified population of GFP$^+$ cells was obtained without later emergence of RFP$^+$ cells. Bar=100 μm. (***B***) Representative dot plot showing that 85% of cells were GFP$^+$ at the time of sorting and 15% were RFP$^+$ that included either non-recombined medial cells or contaminating intimal and adventitial cells. (***C***) Histogram showing % GFP$^+$ and RFP$^+$ cells averaged from 5 independent isolations.

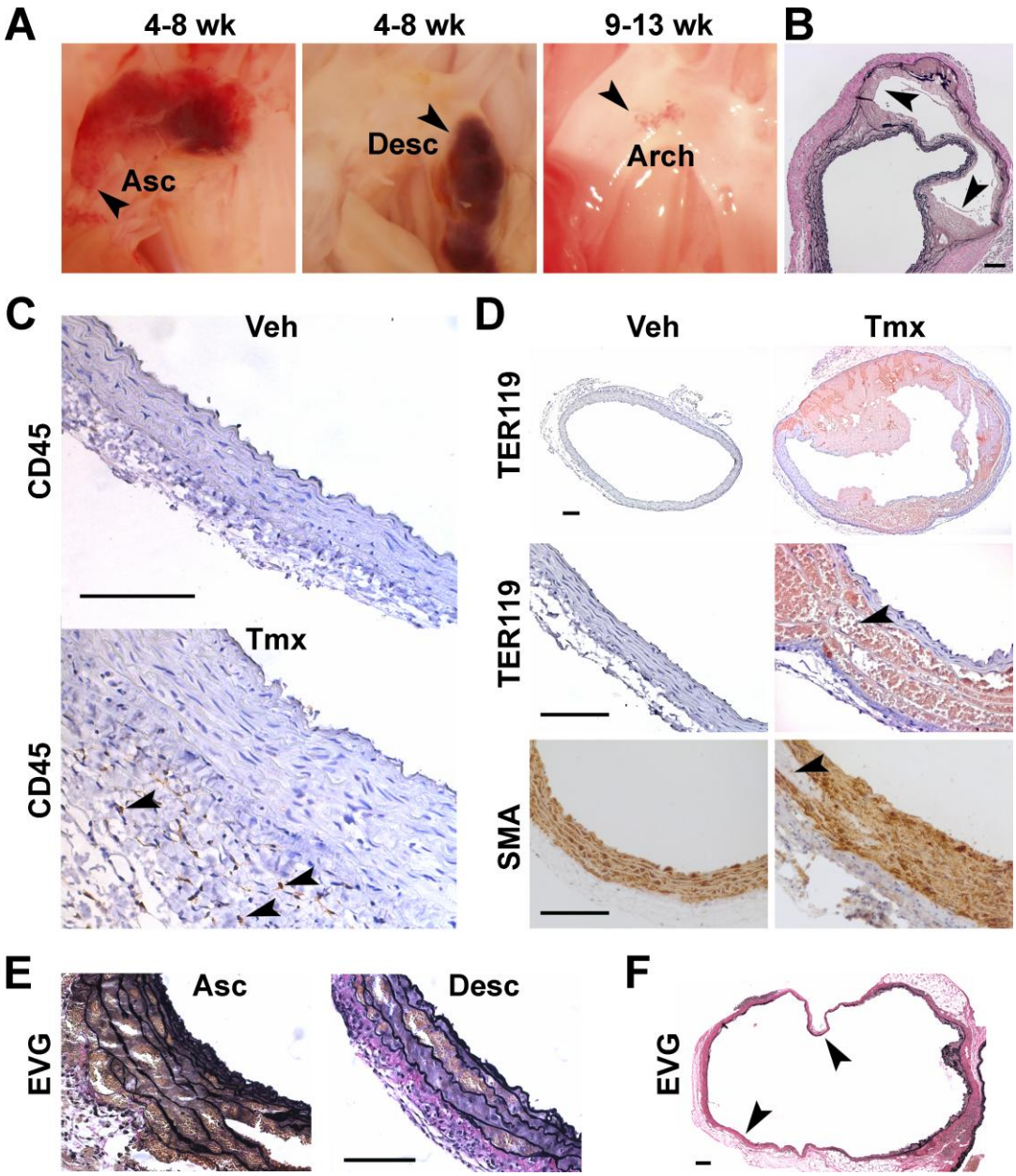

Figure S2. Aortic pathology after *Tgfbr2* disruption. *Myh11-CreER^{T2}.Tgfbr2$^{f/f}$* mice were treated with tamoxifen or vehicle at 4 wk of age (unless otherwise specified) and the thoracic aortas were subsequently analyzed. (***A***) Initiation site and extent of aortic dissections (arrows) at 8 wk (induced at 4 wk) vs. 13 wk (induced at 9 wk of age). (***B***) Obvious false lumen containing blood (arrows) at 8 wk caused by marked separation of elastic laminae. (***C***) Immunohistochemistry for leukocyte common marker, CD45 demonstrated numerous infiltrating cells (arrows) in the adventitia, but not the media, of dissected aortas at 10 wk. (***D***) Immunolabeling for erythroid lineage marker, TER119 and smooth muscle marker, SMA showed many red blood cells within the elastic lamina (arrow) and focal areas of the media devoid of SMCs (arrow) in dissected aortas at 10 wk. (***E***) EVG stains show similar abnormalities of medial hematomas, elastin fragmentation, and elastic lamina widening in both ascending and descending thoracic aorta at 8 wk. (***F***) Extreme degree of medial degeneration with focal areas of vessel wall consisting only of fibrotic adventitia (arrows) at 30 wk. Bars=100 μm.

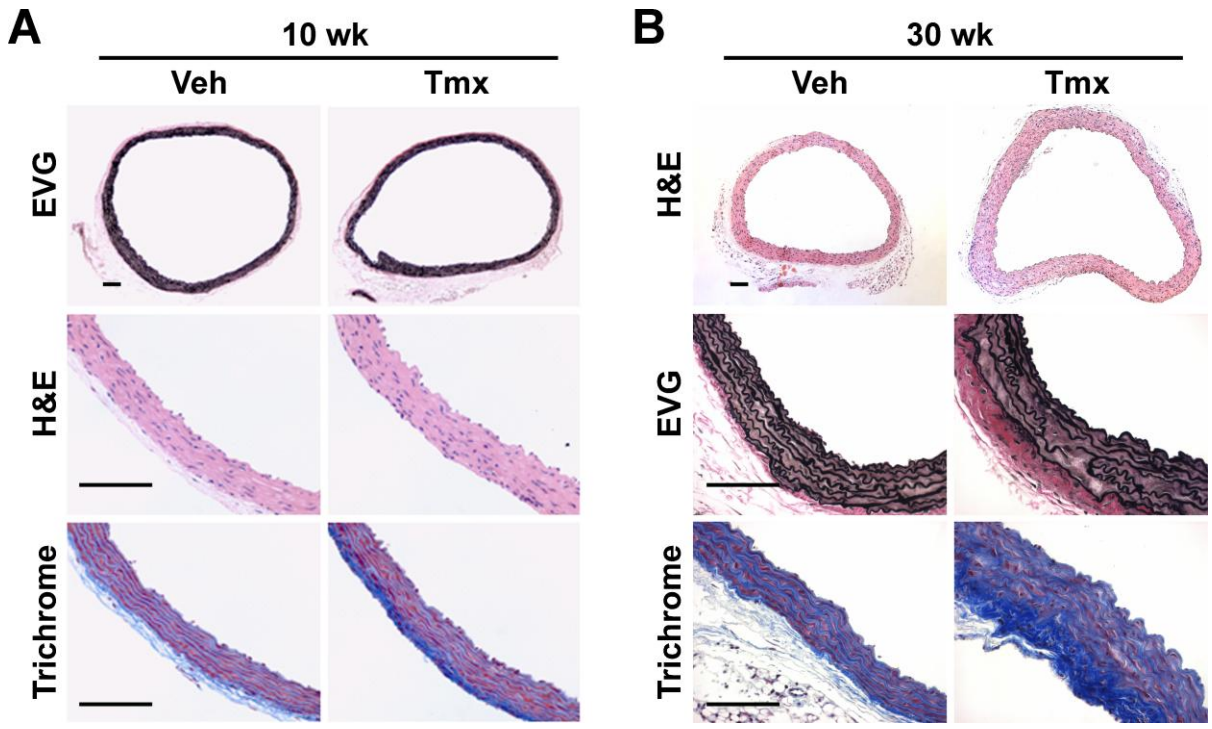

Figure S3. Delayed vascular pathology in the absence of dissection. *Myh11-CreER^{T2}.Tgfbr2$^{f/f}$* mice were treated with vehicle or tamoxifen at 4 wk of age and ascending thoracic aortas without mural hematomas were subsequently analyzed. (***A***) H&E, EVG, and trichrome stains showed relatively normal histological appearance at 10 wk, (***B***) but evidence of elastin fragmentation, elastic lamina widening, and adventitial fibrosis contributing to mural thickening by 30 wk of age. Bars=100 µm.

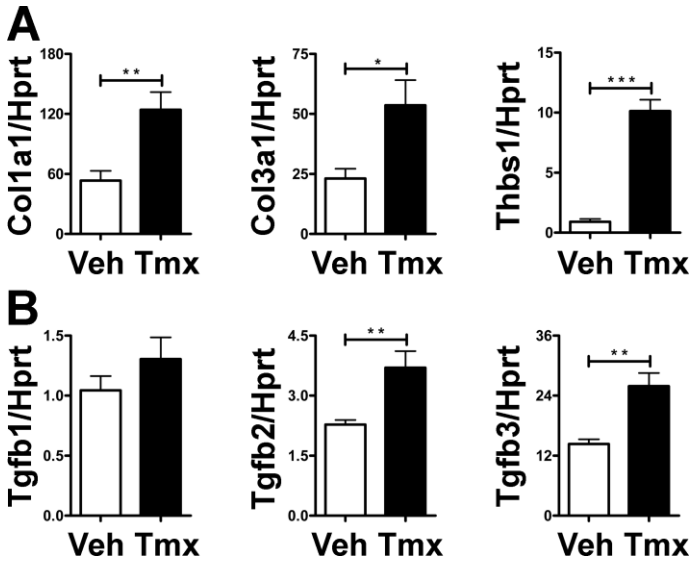

Figure S4. TβRII inactivation in SMCs increases the production of extracellular matrix molecules and TGF-β ligand. Quantitative RT-PCR of thoracic aortas from 6 wk old vehicle- or tamoxifen-treated *Myh11-CreER*^{T2}*.Tgfbr2*$^{f/f}$ mice for (***A***) Col1a1, Col3a1, Thbs1, (***B***) Tgfb1, Tgfb2, and Tgfb3 transcripts; *n*=3-9 pooled from 3 separate experiments; **P*<0.05, ***P*<0.01, and ****P*<0.001, t-test.

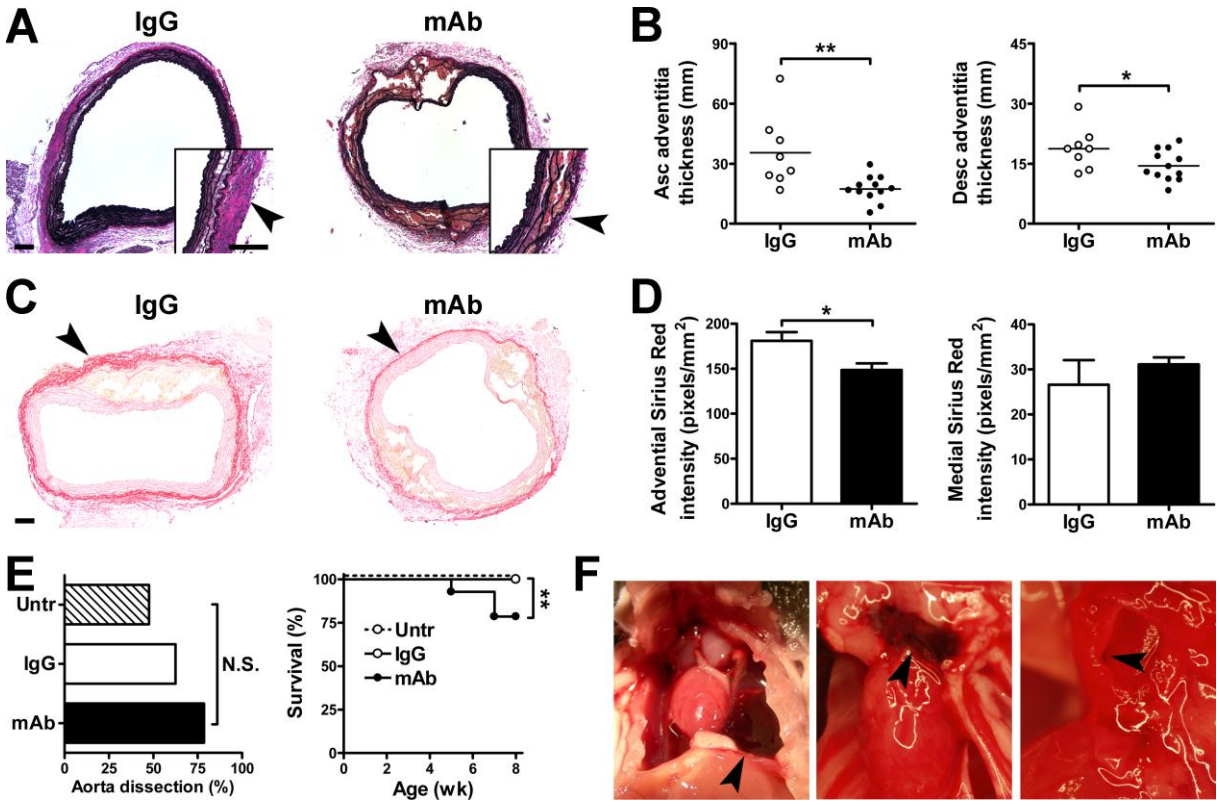

Figure S5. Serologic neutralization of TGF-β after *Tgfbr2* disruption in SMCs does not rescue the aortic dissection phenotype, but prevents adventitial thickening and precipitates fatal aortic rupture. *Myh11-CreER*^{T2}*.Tgfbr2*$^{f/f}$ mice were treated with tamoxifen at 4 wk of age for 5 d and either neutralizing monoclonal antibody (mAb) to TGF-β1, -2, -3 or irrelevant IgG1 at 250 µg i.p., every other day, from 4-8 wk. (***A***) Representative EVG stains of ascending thoracic aortas showing adventitial collagen (red-purple color, arrows) with higher magnification shown in insets; bars=100 µm with (***B***) mean adventitial thickness of ascending and descending aortas; *n*=8 IgG and *n*=14 mAb, **P*<0.05, ***P*<0.01, t-test. (***C***) Representative Sirius Red stains of ascending thoracic aortas showing adventitial collagen (dark red color, arrows); bar=100 µm with (***D***) intensity of Sirius Red signal in adventitia and media of ascending aortas; *n*=7 IgG and *n*=8 mAb, **P*<0.05, t-test. (***E***) Aortic dissection rates of mAb- vs. IgG-treated (littermate controls) or untreated (historical controls) *Tgfbr2* KO mice (11/14 vs. 5/8 vs. 19/40, respectively; *P*=0.1219, chi-square test) and survival rates of mAb- vs. IgG-treated or untreated *Tgfbr2* KO mice (11/14 vs. 8/8 vs. 40/40, respectively; *P*=0.0063, logrank test) at 8 wk of age. (***F***) Post-mortem of mAb-treated mouse at 7 wk showing intra-thoracic blood clot (arrow, left panel), mediastinal hematoma overlying proximal aorta (arrow, middle panel), and free rupture of the underlying ascending aorta (arrow, right panel).

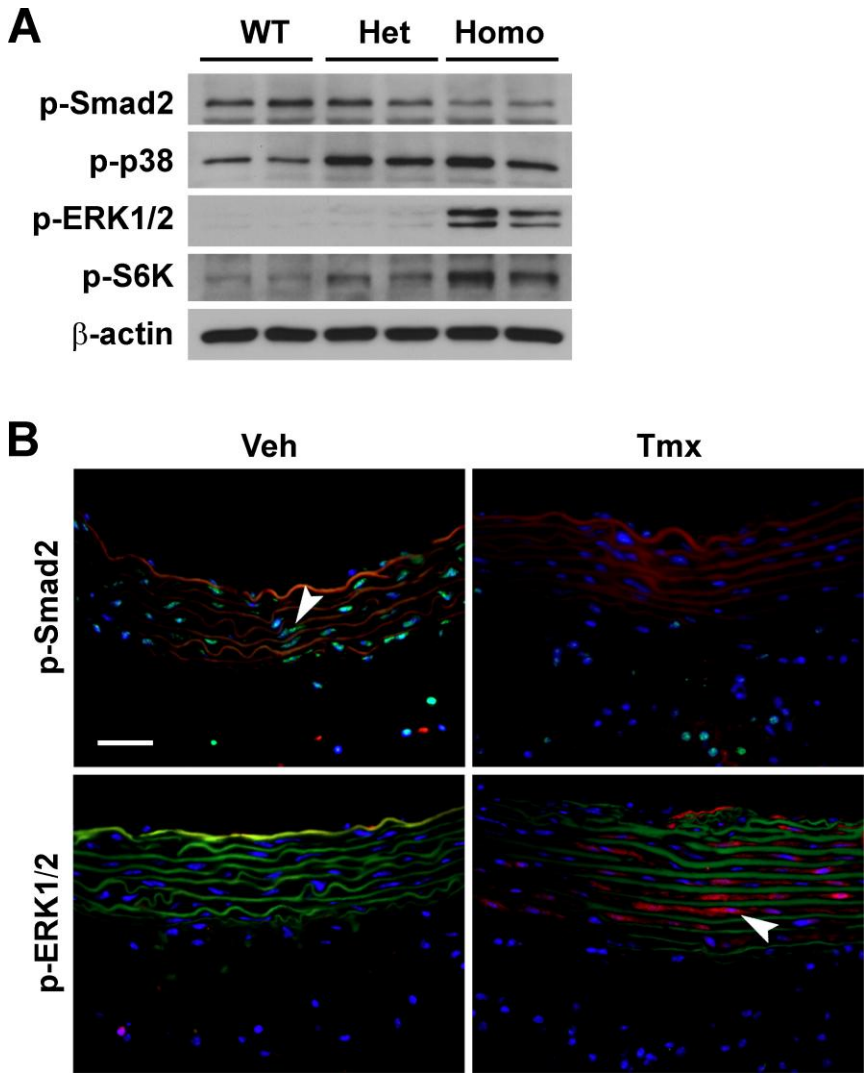

Figure S6. Changes in TGF-β signaling after TβRII inactivation. (***A***) Immunoblotting for phospho-Smad2, phospho-p38, phospho-ERK1/2, and phospho-S6K in thoracic aortas from vehicle-treated *Myh11-CreER^{T2}.Tgfbr2$^{f/f}$* (WT) or tamoxifen-treated *Myh11-CreER^{T2}.Tgfbr2$^{wt/f}$* (Het) and *Myh11-CreER^{T2}.Tgfbr2$^{f/f}$* (Homo) mice at 6 wk. (***B***) Immunofluorescence microscopy for expression of phospho-Smad2 (green color as indicated by arrow with blue color for DAPI labeling of nuclei and red autofluorescence of elastic lamina delineating the media in the upper two panels) and phospho-ERK1/2 (red color as indicated by arrow with blue color for DAPI labeling of nuclei and green autofluorescence of elastic lamina delineating the media in the lower two panels) in the thoracic aorta wall of vehicle- or tamoxifen-treated *Myh11-CreER^{T2}.Tgfbr2$^{f/f}$* mice at 10 wk; bar=30 μm.

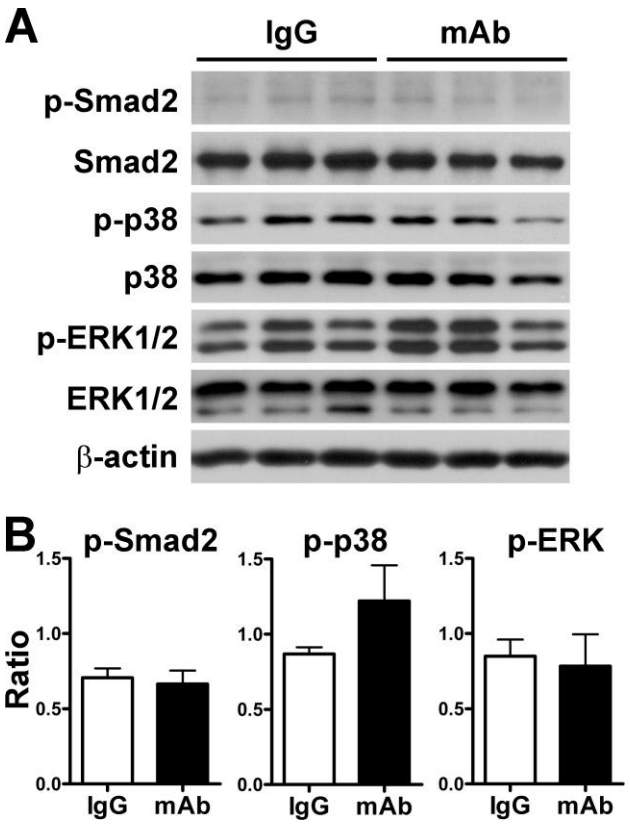

Figure S7. Serologic neutralization of TGF-β does not further inhibit Smad2 phosphorylation nor prevent MAPK activation in KO aorta. (***A***) Representative immunoblotting and (***B***) relative expression of phosphorylated (p-) to total Smad2, p38, and ERK1/2 in thoracic aortas from *Myh11-CreER*^{T2}*.Tgfbr2*$^{f/f}$ mice treated with tamoxifen at 4 wk for 5 d and either neutralizing monoclonal antibody (mAb) to TGF-β1, -2, -3 or irrelevant IgG1 at 250 μg i.p., q.o.d., from 4-6 wk; *n*=6; *P*=0.7025 for p-Smad2, *P*=0.1755 for p-p38, *P*=7853 for p-ERK1/2, t-test.

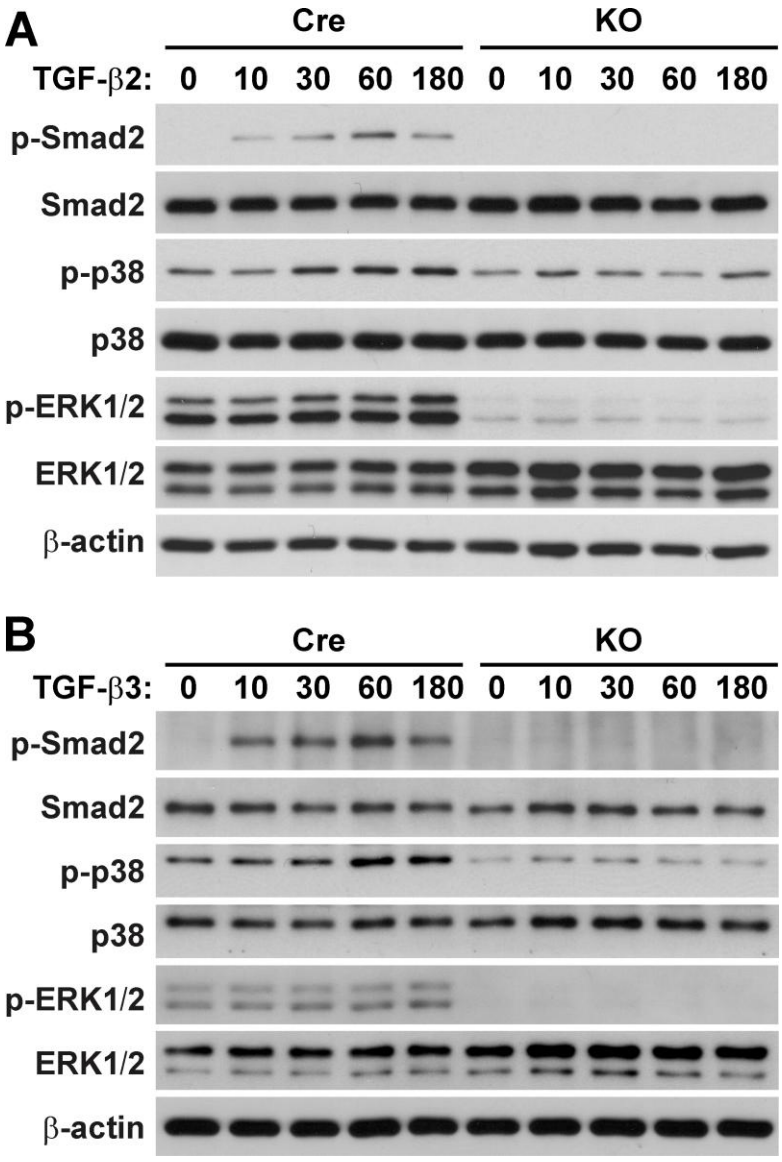

Figure S8. Disruption of TβRII in cultured SMCs prevents signaling to multiple TGF-β isoforms. (***A***) Immunoblotting for phosphorylated (p-) and total Smad2, p38, and ERK1/2 in purified GFP^{+} SMCs isolated from the thoracic aortas of tamoxifen-induced *mT/mG.Myh11-CreER*^{T2} (Cre) and *mT/mG.Myh11-CreER*^{T2}*.Tgfbr2*$^{f/f}$ (KO) mice, serum-deprived for 24 h, and then treated with TGF-β2 at 1 ng/mL or (***B***) TGF-β3 at 1 ng/mL for 0-180 min.

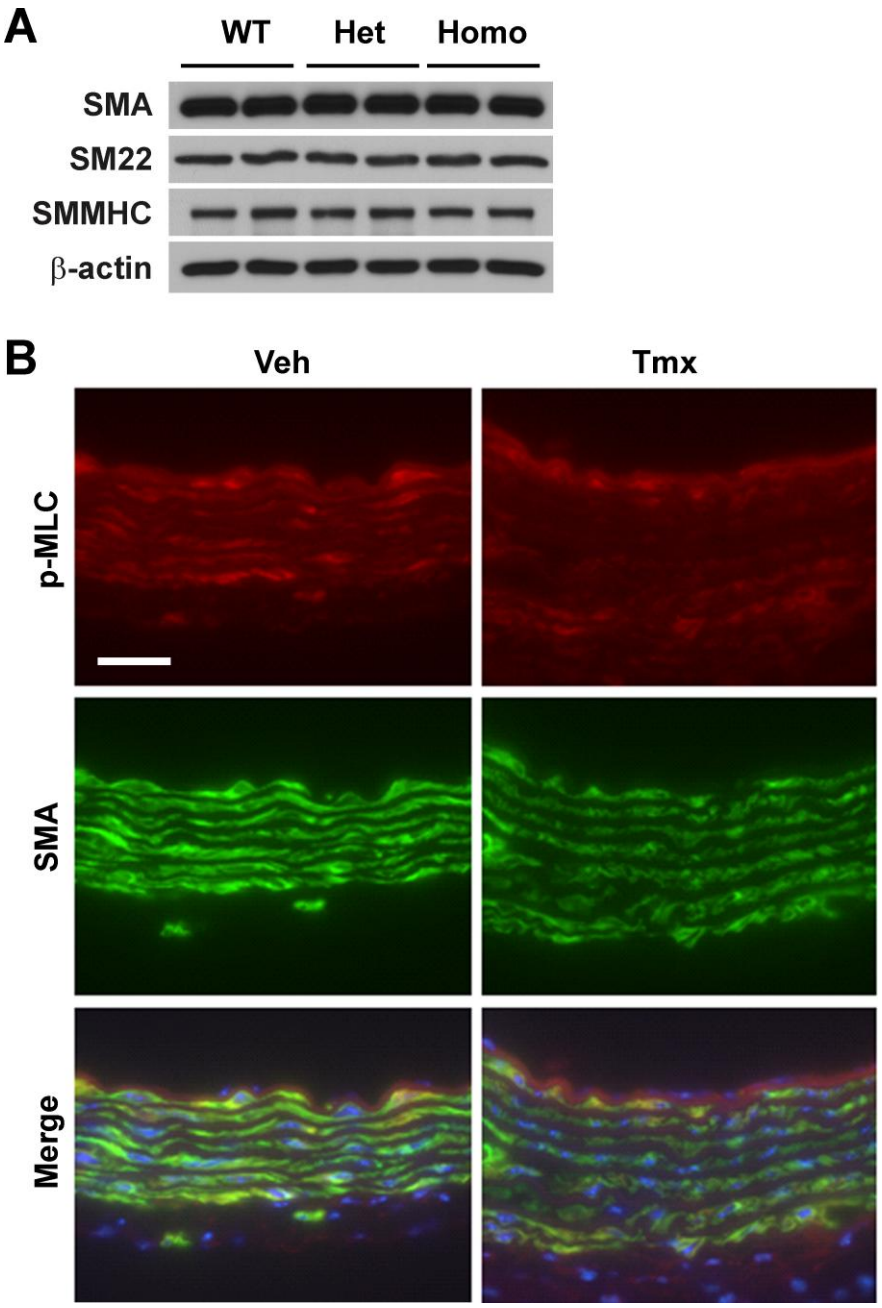

Figure S9. Changes in smooth muscle contractile proteins after TβRII inactivation. (***A***) Immunoblotting for SMA, SM22, and SMMHC in thoracic aortas from vehicle-treated *Myh11-CreER^{T2}.Tgfbr2$^{f/f}$* (WT) or tamoxifen-treated *Myh11-CreER^{T2}.Tgfbr2$^{wt/f}$* (Het) and *Myh11-CreER^{T2}.Tgfbr2$^{f/f}$* (Homo) mice at 6 wk. (***B***) Immunofluorescence microscopy for phospho-MLC (red color) and SMA (green color) with merged images including DAPI labeling of nuclei (blue color) in the aortic wall of vehicle- or tamoxifen-treated *Myh11-CreER^{T2}.Tgfbr2$^{f/f}$* mice at 10 wk; bar=30 μm.

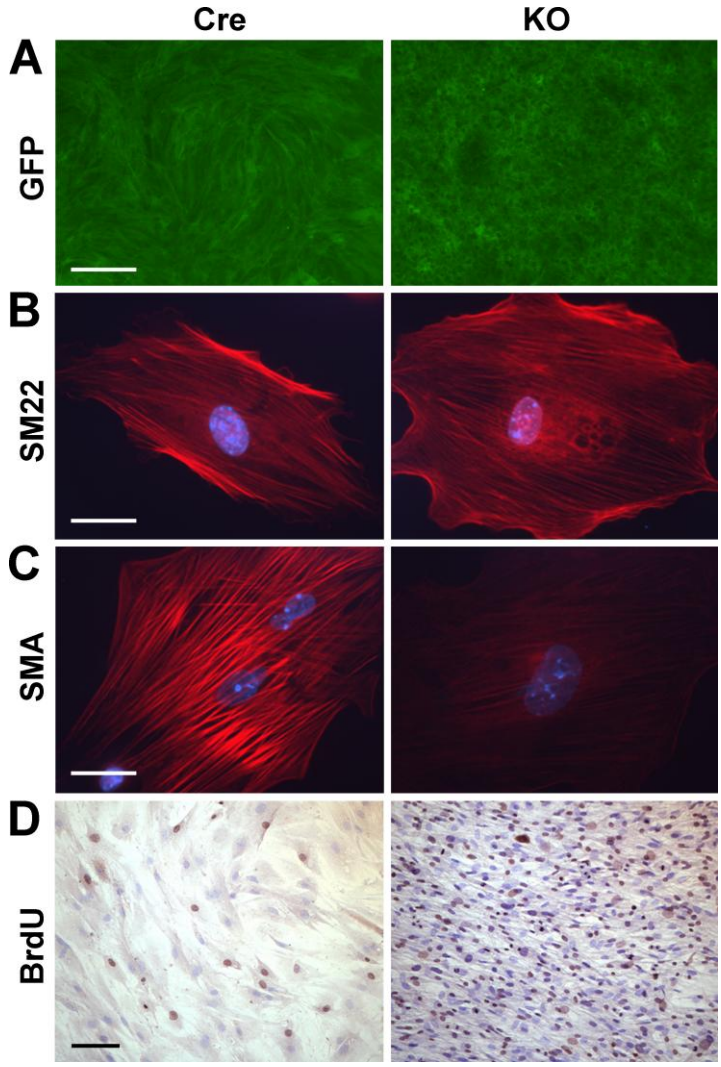

Figure S10. Shift from contractile to proliferative phenotype after *Tgfbr2* disruption. SMCs were cultured from the thoracic aortas of tamoxifen-induced *mT/mG.Myh11-CreER*^{T2} (Cre) or *mT/mG.Myh11-CreER*^{T2}*.Tgfbr2*$^{f/f}$ (KO) mice. (***A***) Appearance of flow cytometry-selected GFP^{+} (green color) cells at passage 6; bar=100 μm. Immunofluorescence analysis for (***B***) SM22 and (***C***) SMA expression (red color); bars=30 μm. (***D***) SMCs were plated at 1x10^{4} cells/mm^{2} in serum-supplemented Claycomb medium, cultured for 24 h, then BrdU was added at 1 mM for 24 h, and its incorporation in fixed permeabilized cells was assessed by immunohistochemistry (brown color, nuclei counter-stained with hematoxylin); bar=100 μm.

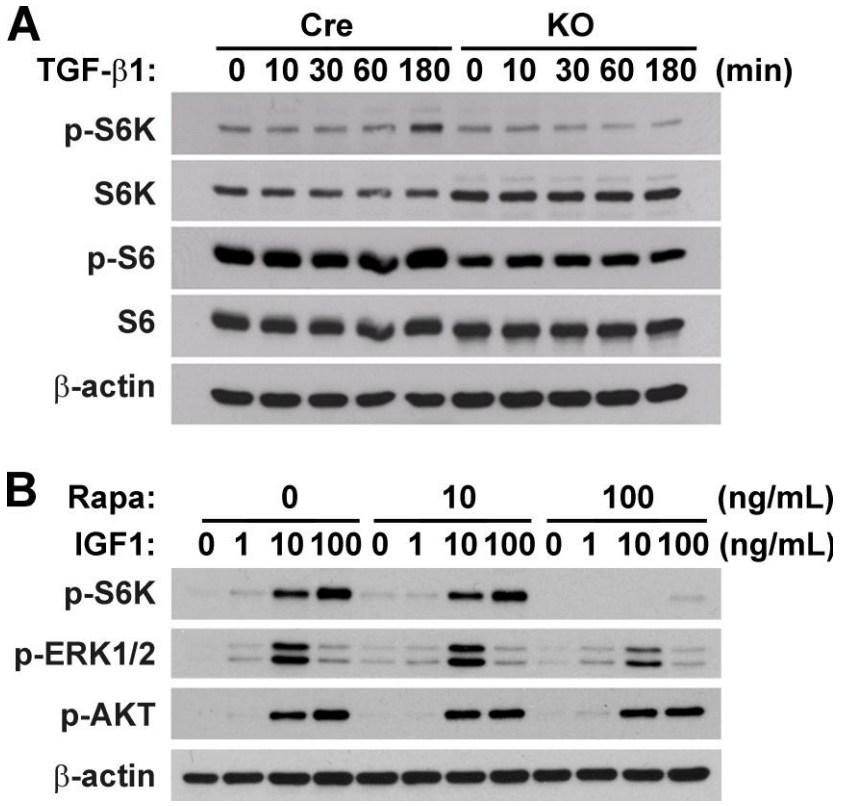

Figure S11. Delayed mTOR signaling by TGF-β and effects of mTOR inhibition on IGF1 signaling. (***A***) Immunoblotting for phospho- and total S6K and S6 in aortic GFP^{+} SMCs from tamoxifen-induced *mT/mG.Myh11-CreER^{T2}* (Cre) or *mT/mG.Myh11-CreER^{T2}.Tgfbr2$^{f/f}$* (KO) mice, serum-deprived for 24 h, and then treated with TGF-β1 at 1 ng/mL for 0-180 min. Increased activation of mTOR mediators (S6K and S6) is evident at 180 min only in TβRII-expressing (Cre) SMCs. (***B***) Immunoblotting for phospho-S6K, phospho-ERK1/2, and phospho-AKT in aortic GFP^{+} SMCs lacking TβRII from KO mice, serum-deprived for 24 h, pretreated with rapamycin at 0-100 ng/mL for 60 min and then treated with IGF1 at 0-100 ng/mL for 10 min. Only IGF1 signaling mediators downstream of mTOR (S6K) are inhibited by rapamycin.

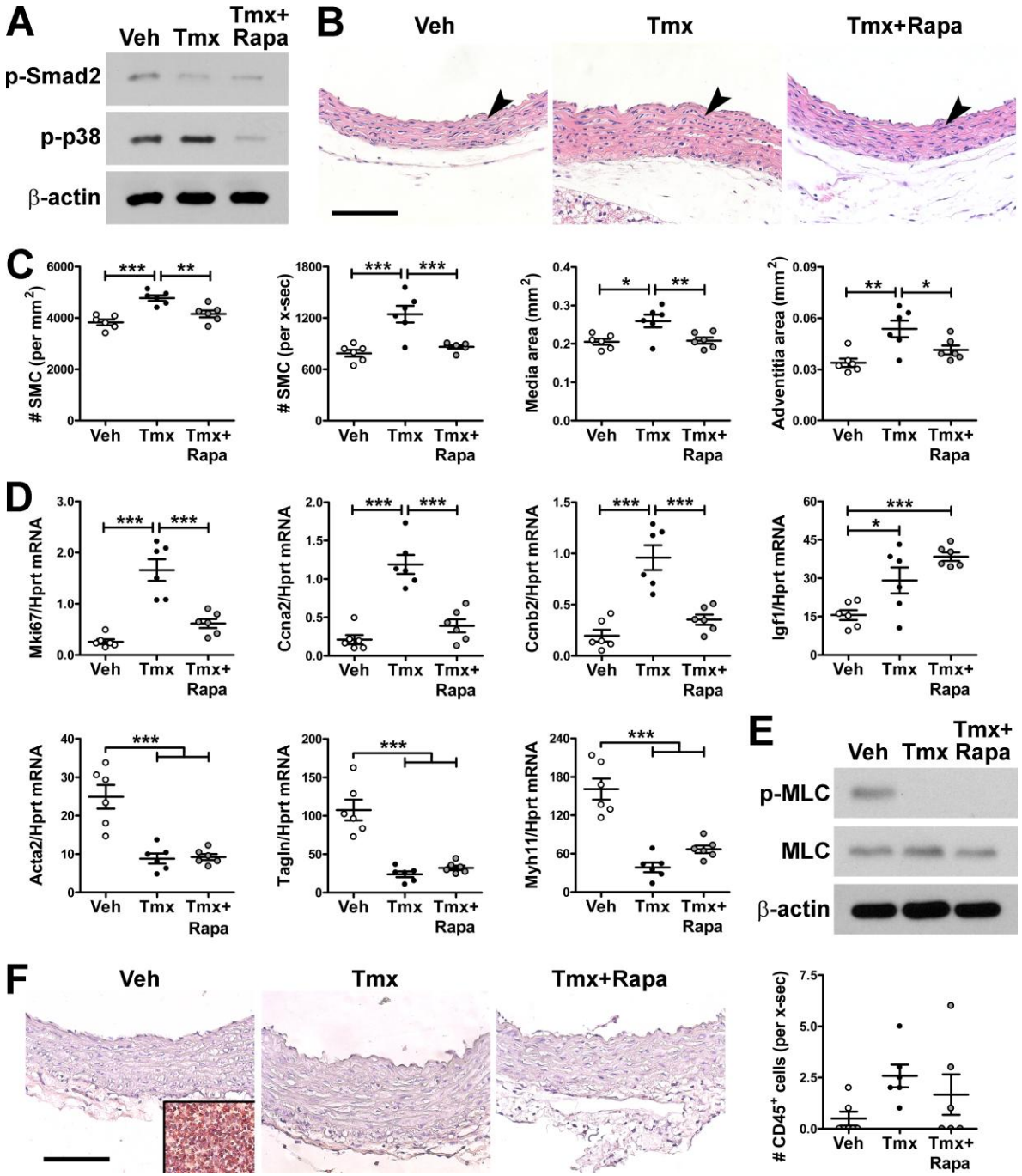

Figure S12. Rapamycin maintains a quiescent SMC phenotype. Thoracic aortas were analyzed from *Myh11-CreER^{T2}.Tgfbr2$^{f/f}$* mice treated with vehicle or tamoxifen ± rapamycin at 2 mg/kg/d i.p. q.d. from 3-7 wk. (***A***) Immunoblotting for phospho-Smad2 and -p38. (***B***) H&E stains showing nuclei (blue color, arrows); bar=100 μm. (***C***) Number of medial nuclei per mm^2 or per cross-section (x-sec), media and adventitia areas; *n*=6, **P*<0.05, ***P*<0.01, ****P*<0.001, one-way ANOVA. (***D***) qPCR for transcript expression of proliferative marker (Mki67), cell cycle regulators (Ccna2, Ccnb2), growth factor (Igf1), and contractile molecules (Acta2, Tagln, Myh11); *n*=6, **P*<0.05, ****P*<0.001, one-way ANOVA. (***E***) Immunoblotting for phospho-MLC and MLC. (**F**) Immunohistochemistry for CD45 (inset: spleen as positive control) showing similar sparse leukocytes in adventitia of untreated and treated groups (*n*=6, *P*=0.1311, one-way ANOVA) and uniformly absent medial infiltrates; bar=100 μm.

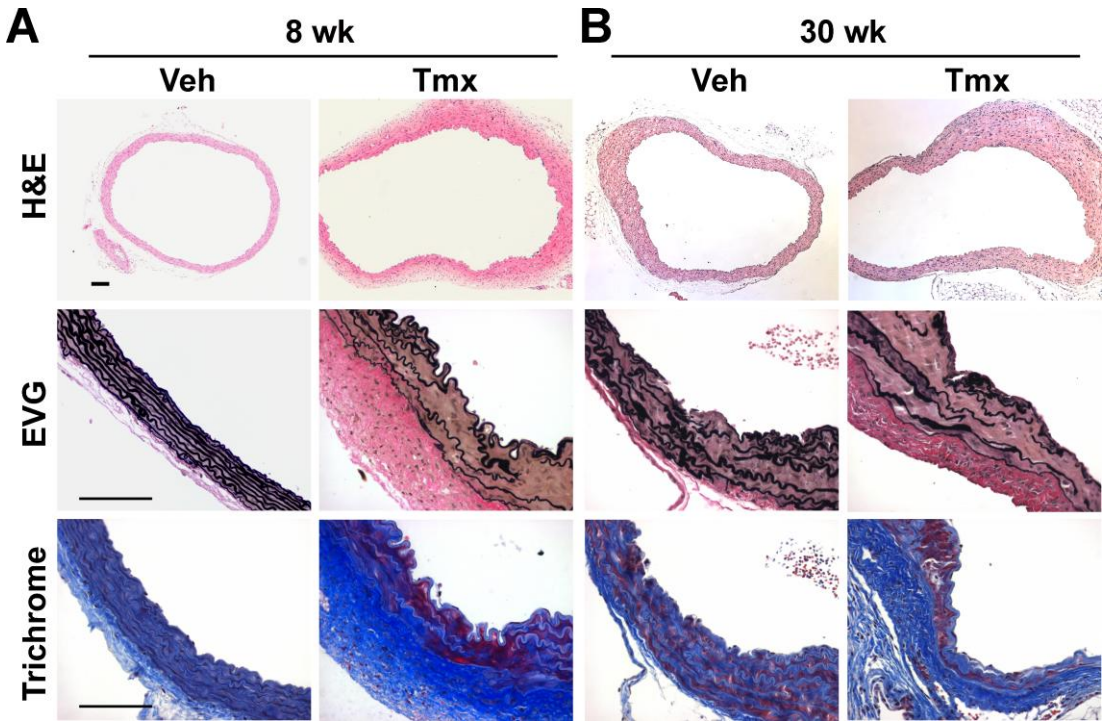

Figure S13. TβRII inactivation in smooth muscle exacerbates aortic medial degeneration induced by mutant fibrillin-1. (***A***) H&E, EVG, and trichrome stains of ascending thoracic aortas from 8 wk old *Fbn1*$^{C1039G/+}$*.Myh11-CreER*^{T2}*.Tgfbr2*$^{f/f}$ mice showed greater elastin disruption, increased adventitial fibrosis, and thicker vessel walls after tamoxifen than vehicle treatment at 4 wk of age. (***B***) Similarly, histological analysis at 30 wk of age showed greater pathological changes of the aorta following *Tgfbr2* disruption on *Fbn1*$^{C1039G/+}$ background than due to mutant *Fbn1* alone. Bars=100 μm.

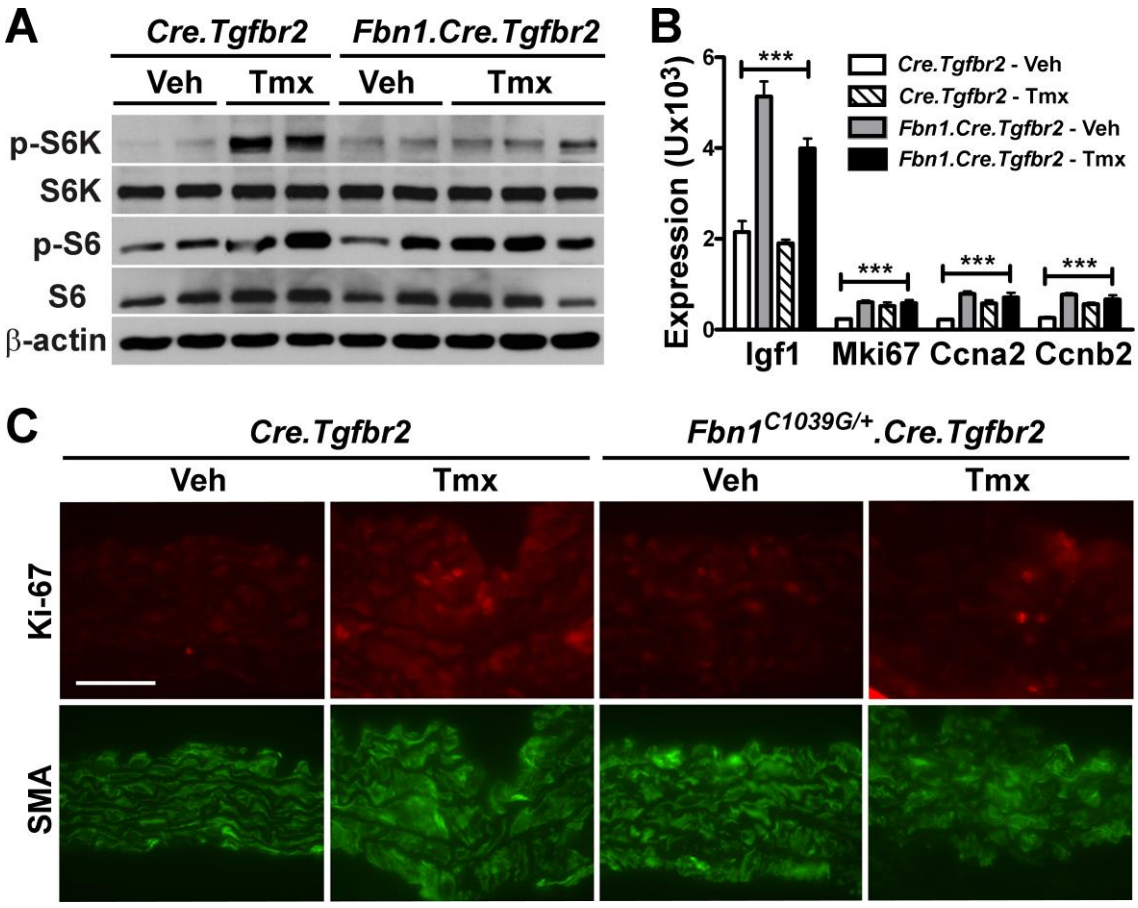

Figure S14. Effects of TβRII inactivation and/or fibrillin-1 mutation in thoracic aorta at 5-8 wk of age. *Myh11-CreER^{T2}.Tgfbr2$^{f/f}$* (abbreviated as *Cre.Tgfbr2*) mice were cross-bred to *Fbn1$^{C1039G/+}$* (abbreviated as *Fbn1*) mice, treated with vehicle or tamoxifen for 5 d starting at 4 wk, and their aortas were analyzed at various ages. (***A***) Immunoblotting for phospho- and total S6K and S6 in thoracic aortas at 5 wk. (***B***) Microarray expression data (in arbitrary units) for growth factor, proliferative marker, and cell cycle regulators in thoracic aortas at 6 wk; n=3, ***P<0.001, one-way ANOVA. (***C***) Immunofluorescence analysis for the proliferative marker, Ki-67 (red color) and the smooth muscle marker, SMA (green color) in thoracic aortas at 8 wk; bar=50 μm. Signaling and expression changes (increased p-S6K and p-S6, increased Igf1, increased proliferation markers and cell cycle regulators) characteristic of *Tgfbr2* deletion in aortic smooth muscle were not greater in compound mutant animals.

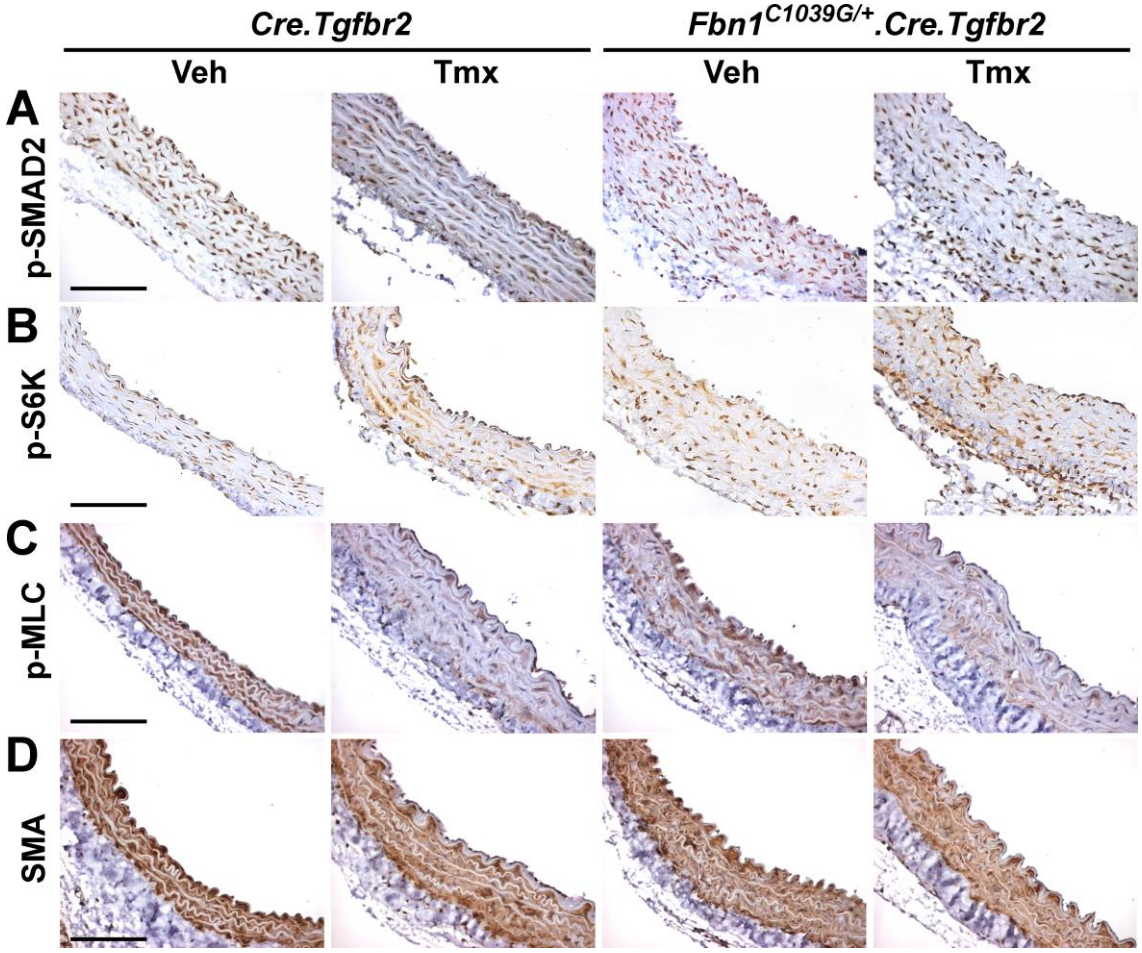

Figure S15. Effects of TβRII inactivation and/or fibrillin-1 mutation on thoracic aorta at 30 wk of age. *Myh11-CreER^{T2}.Tgfbr2$^{f/f}$* (abbreviated as *Cre.Tgfbr2*) mice were cross-bred to *Fbn1$^{C1039G/+}$* mice, treated with vehicle or tamoxifen for 5 d starting at 4 wk, and their thoracic aortas were procured at 30 wk. Immunohistochemical analysis for (***A***) phospho-Smad2, (***B***) phospho-S6K, (***C***) phospho-MLC, and (***D***) SMA; protein detection indicated by brown color, bars=100 μm. Signaling and expression changes (decreased p-Smad2, increased p-S6K, decreased p-MLC, and decreased SMA) characteristic of *Tgfbr2* deletion in aortic smooth muscle were not greater in compound mutant animals.

Table S1. Microarray analysis of ascending aortas from 6 wk old *Myh11-CreER^{T2}.Tgfbr2$^{f/f}$* mice treated with vehicle or tamoxifen at 4 wk of age.

Transcript ID	Gene assigned	Gene symbol	Fold-Δ Tmx/Veh	P-value Tmx/Veh	FDR adj. P-value	Mean Veh	Mean Tmx	Veh 1	Veh 2	Veh 3	Tmx 4	Tmx 5	Tmx 6
10414262	NM_007895	Ear2	4.77	0.000224	0.000379	167.2	798.0	172	138	197	628	651	1243
10496727	NM_026995	Ddah1	4.59	0.000093	0.000204	329.2	1510.2	277	309	417	1607	1167	1837
10523717	NM_009263	Spp1	4.16	0.001223	0.001646	185.6	771.9	200	278	115	1043	617	715
10379535	NM_021443	Ccl8	3.66	0.000009	0.000044	115.9	424.3	102	116	132	384	347	574
10474700	NM_011580	Thbs1	3.63	0.000220	0.000379	2822.6	10246.9	2399	2989	3136	10372	8972	11562
10499189	NM_030707	Fcrls	3.55	0.000000	0.000007	374.6	1331.2	343	353	433	1263	1320	1414
10450374	L78788 // D	D17H6S56E	3.55	0.000001	0.000010	214.0	760.5	205	211	226	774	673	845
10497831	NM_009828	Ccna2	3.52	0.000038	0.000125	223.2	785.3	217	203	253	758	714	895
10423836	NM_026778	Cthrc1	3.50	0.000001	0.000009	480.7	1680.2	455	497	491	1965	1532	1575
10605848	NM_177789	Vsig4	3.44	0.000958	0.001302	144.9	498.0	100	188	161	403	592	517
10398075	NM_009252	Serpina3n	3.27	0.000004	0.000030	2912.0	9528.3	3146	2985	2630	9884	10103	8663
10555323	NM_177161	P4ha3	3.20	0.000166	0.000301	253.7	811.3	232	344	205	909	629	935
10443690	NM_021332	Glp1r	3.16	0.000002	0.000014	188.2	595.6	195	181	189	511	578	715
10440091	NM_007739	Col8a1	3.11	0.000183	0.000325	1208.4	3757.4	1153	1496	1023	4130	3761	3416
10420935	NM_007940	Ephx2	3.08	0.000039	0.000125	548.9	1691.5	663	594	420	1855	1388	1879
10379727	NM_001081	Gm11428	3.04	0.000372	0.000585	1061.6	3225.7	861	1006	1381	2738	3356	3653
10594774	NM_007630	Ccnb2	3.01	0.000010	0.000047	256.6	773.6	238	239	297	755	739	831
10348902	NM_199366	Gal3st2	3.00	0.000005	0.000030	501.6	1504.7	568	501	443	1532	1493	1490
10598976	NM_001044	Timp1	2.91	0.000008	0.000044	1363.1	3972.7	1211	1569	1332	4200	4358	3425
10348896	NM_199366	Gal3st2	2.85	0.000008	0.000044	306.4	874.0	348	307	269	915	902	809
10562637	NM_172301	Ccnb1	2.83	0.000087	0.000194	147.2	416.4	132	185	131	385	403	466
10391504	NM_010791	Meox1	2.82	0.000000	0.000002	323.3	911.7	291	348	334	945	908	884
10419156	NM_053112	Ear10	2.81	0.000051	0.000135	139.0	390.6	149	126	143	356	332	503
10587799	NM_008880	Plscr2	2.76	0.000009	0.000044	339.4	936.6	353	398	278	999	895	919
10466210	NM_026835	Ms4a6d	2.74	0.000360	0.000573	320.5	878.9	328	288	348	1130	776	774
10360406	NM_172648	Ifi205	2.71	0.001973	0.002568	269.6	730.6	295	380	174	848	709	648
10404606	NM_010745	Ly86	2.71	0.000041	0.000125	784.1	2124.5	785	723	849	2384	1756	2291
10554445	NM_145150	Prc1	2.67	0.000081	0.000184	154.2	412.1	165	153	146	358	405	483
10389222	NM_009139	Ccl6	2.66	0.000303	0.000493	535.3	1424.2	512	462	647	1204	1582	1517
10512470	NM_001110	Cd72	2.64	0.003694	0.004618	348.8	920.7	270	419	375	1600	643	758
10466200	NM_027836	Ms4a7	2.62	0.000134	0.000254	207.5	544.2	178	225	224	686	411	571
10390707	NM_011623	Top2a	2.62	0.000102	0.000216	166.9	437.3	147	193	164	422	391	507
10568714	NM_001081	Mki67	2.60	0.000134	0.000254	230.1	598.4	232	245	215	587	546	668
10411739	NM_172301	Ccnb1	2.59	0.000059	0.000148	110.2	285.7	112	126	95	269	280	310
10515836	NM_172301	Ccnb1	2.57	0.000130	0.000253	85.8	220.7	89	100	71	216	227	219
10598175	NM_053112	Ear10	2.57	0.000073	0.000170	140.8	361.8	151	127	146	318	316	472
10494271	NM_021281	Ctss	2.55	0.000001	0.000012	626.0	1596.2	616	661	603	1864	1354	1612
10484307	NM_011356	Frzb	2.51	0.000016	0.000069	1500.4	3772.0	1720	1643	1195	3870	3543	3914
10365559	NM_010512	Igf1	2.41	0.000026	0.000102	2122.3	5118.5	2108	1754	2585	4870	4758	5788
10501063	NM_007651	Cd53	2.41	0.000002	0.000013	474.9	1142.4	456	504	466	1193	1097	1139
10513818	NM_019641	Stmn1	2.40	0.000037	0.000125	633.7	1521.0	711	629	569	1524	1354	1706
10419154	NM_007894	Ear1	2.39	0.000380	0.000589	142.7	341.0	147	126	157	281	308	459
10410386	AK149411 /	E430024C0	2.38	0.006039	0.007289	88.6	210.8	103	77	88	251	134	279
10410388	AK149411 /	E430024C0	2.38	0.006039	0.007289	88.6	210.8	103	77	88	251	134	279
10590631	NM_009915	Ccr2	2.37	0.000036	0.000125	88.6	210.2	86	101	80	256	218	167
10461622	NM_027209	Ms4a6b	2.36	0.000433	0.000651	281.4	665.1	315	245	288	807	620	588
10404439	NM_011452	Serpinb9b	2.36	0.000042	0.000125	136.2	321.6	136	125	149	287	314	370
10508986	NM_019641	Stmn1	2.35	0.000046	0.000132	701.4	1651.8	810	692	616	1652	1498	1821
10470392	NM_029981	Adamtsl2	2.34	0.000002	0.000015	2382.6	5573.2	2637	2292	2237	5568	5758	5399
10601385	NM_205826	Tlr13	2.34	0.000023	0.000091	342.6	800.3	332	378	320	931	694	793
10363070	NM_008147	Gp49a	2.33	0.000007	0.000042	269.8	629.9	236	311	268	696	604	594
10446282	NM_010130	Emr1	2.33	0.000001	0.000010	593.4	1384.2	546	601	637	1435	1274	1451
10586448	NM_026515	2810417H1	2.32	0.000057	0.000145	134.9	313.2	139	132	133	325	302	314
10595211	NM_007730	Col12a1	2.32	0.000022	0.000089	488.9	1133.8	448	448	582	1234	1184	997
10530441	NM_016869	Corin	2.31	0.002080	0.002672	679.7	1573.4	717	780	561	2025	1606	1198
10541564	NM_153197	Clec4a3	2.31	0.000041	0.000125	194.0	448.7	178	223	184	443	366	557
10607868	NM_133212	Tlr8	2.29	0.000001	0.000010	270.8	620.3	288	248	278	614	595	654
10503241	NM_013526	Gdf6	2.29	0.000070	0.000170	364.8	834.4	366	351	377	848	680	1007
10603099	NM_010216	Figf	2.28	0.000038	0.000125	1327.3	3026.0	1486	1117	1409	2930	3015	3138

Transcript ID	Gene assigned	Gene symbol	Fold-Δ Tmx/Veh	P-value Tmx/Veh	FDR adj. P-value	Mean Veh	Mean Tmx	Veh 1	Veh 2	Veh 3	Tmx 4	Tmx 5	Tmx 6
10360382	NM_00832	Ifi204	2.28	0.008943	0.010347	225.6	514.3	198	209	278	894	382	398
10461614	NM_02859	Ms4a6c	2.28	0.000641	0.000906	645.1	1469.5	740	541	670	1821	1287	1354
10403834	NM_01668	Sfrp4	2.27	0.000606	0.000866	856.6	1942.6	770	700	1166	1943	1633	2311
10551197	NM_00999	Cyp2b10	2.26	0.014191	0.016003	556.6	1256.5	823	459	457	1369	1106	1311
10360377	BC150711	AI607873	2.26	0.000912	0.001251	800.4	1805.6	775	759	871	1992	1488	1986
10600857	NM_01041	Heph	2.25	0.000000	0.000007	260.5	585.7	284	243	256	550	575	636
10428604	NM_00876	Tnfrsf11b	2.25	0.000001	0.000009	978.7	2198.5	973	956	1008	2126	2185	2287
10541555	NM_19931	Clec4a1	2.24	0.000048	0.000133	265.6	595.8	295	238	267	602	594	591
10369815	NM_00765	Cdc2a	2.24	0.000242	0.000403	295.4	662.6	274	329	286	665	573	764
10547657	NM_00977	C3ar1	2.24	0.000050	0.000135	731.2	1638.8	672	646	901	1849	1416	1681
10487480	NM_00111	Bub1	2.24	0.000479	0.000699	95.1	213.2	89	105	92	195	194	256
10402435	NM_00845	Serpina3c	2.24	0.000278	0.000458	219.1	490.4	197	220	243	455	433	598
10360028	NM_00107	Fcgr2b	2.24	0.000000	0.000003	646.2	1446.2	618	670	652	1379	1439	1524
10372652	NM_01359	Lyz1	2.20	0.000170	0.000305	463.6	1021.8	413	565	427	934	921	1240
10594251	NM_02424	Kif23	2.20	0.000118	0.000241	198.0	435.4	210	168	219	403	398	514
10462796	NM_01061	Kif11	2.16	0.000072	0.000170	191.6	414.2	188	191	195	408	392	444
10436095	NM_02050	Retnla	2.16	0.016799	0.018666	271.3	586.1	215	230	402	443	505	901
10424543	NM_01886	Wisp1	2.15	0.000032	0.000119	387.7	834.1	369	351	450	801	874	828
10389214	NM_01133	Ccl9	2.15	0.000119	0.000241	504.4	1082.2	514	462	540	1044	1064	1140
10396952	NM_00103	Ttc9	2.12	0.002102	0.002675	458.6	974.4	384	544	462	758	850	1434
10517517	NM_00757	C1qa	2.12	0.000012	0.000056	956.9	2028.5	911	914	1052	2024	1850	2229
10360391	NM_00104	Ifi203	2.11	0.008569	0.010054	462.6	978.3	440	404	558	1416	627	1054
10526783	NM_00101	BC055004	2.11	0.000128	0.000252	143.1	302.1	126	152	153	279	394	250
10603551	NM_00780	Cybb	2.11	0.000030	0.000115	889.3	1876.7	887	910	871	2292	1505	1916
10444291	NM_20710	H2-Ab1	2.11	0.000717	0.001003	1173.6	2473.3	1130	1362	1050	2364	2178	2938
10605815	NM_08085	Asb12	2.11	0.000225	0.000379	172.9	363.9	187	139	200	436	370	299
10387536	NM_00985	Cd68	2.10	0.000192	0.000337	827.6	1737.4	670	844	1002	1763	1509	1971
10587854	NM_17790	Slc9a9	2.09	0.000160	0.000294	467.1	977.9	437	433	539	859	895	1215
10360040	NM_01018	Fcgr3	2.09	0.000000	0.000007	444.4	929.0	421	452	461	934	915	938
10502565	NM_03060	Clca2	2.09	0.005716	0.007019	111.1	232.1	80	137	124	296	239	177
10581013	NM_00986	Cdh11	2.09	0.000125	0.000249	1609.7	3363.2	1825	1769	1292	3157	3419	3524
10377405	NM_01149	Aurkb	2.07	0.000054	0.000139	366.8	760.8	354	380	367	698	743	850
10450242	NM_00978	C4b	2.07	0.000009	0.000044	1451.5	3009.5	1413	1386	1561	2949	3144	2940
10466190	ENSMUST	Ms4a14	2.06	0.000387	0.000589	87.7	181.0	97	79	88	213	157	178
10462623	NM_00833	Ifit1	2.06	0.035871	0.038630	356.0	734.3	310	287	509	1366	503	576
10363082	NM_01353	Lilrb4	2.06	0.000019	0.000079	295.4	607.6	253	336	303	701	542	591
10454709	NM_00900	Kif20a	2.06	0.001691	0.002254	178.3	366.7	173	183	179	331	332	449
10428370	NM_17545	Abra	2.05	0.006738	0.008063	964.7	1976.3	936	1200	800	2026	2572	1481
10557862	NM_00108	Itgam	2.05	0.000000	0.000007	265.0	542.5	252	279	264	567	534	527
10508663	NM_01068	Laptm5	2.04	0.000005	0.000031	1703.4	3479.6	1568	1808	1743	3597	3278	3573
10487340	NM_14481	Ncaph	2.04	0.000000	0.000007	193.3	393.5	201	195	185	379	384	419
10557156	NM_01112	Plk1	2.03	0.000061	0.000149	337.8	687.2	334	344	335	656	637	776
10416437	NM_00887	Lcp1	2.03	0.000040	0.000125	618.8	1254.7	586	682	593	1516	1114	1170
10411082	NM_01158	Thbs4	2.02	0.003950	0.004894	353.9	716.3	317	490	285	759	717	675
10408077	NM_17818	Hist1h2ak	2.02	0.000075	0.000173	1260.4	2547.2	1205	1443	1152	2429	2292	2969
10407126	NM_15280	Plk2	2.02	0.000119	0.000241	191.7	387.0	209	214	158	412	353	399
10434689	NM_01346	Ahsg	2.02	0.006869	0.008149	1147.1	2313.9	1284	1327	885	2678	1676	2760
10517513	NM_00757	C1qc	2.01	0.000469	0.000691	1664.0	3342.5	1402	1572	2090	3451	3146	3440
10485982	NM_00960	Actc1	2.01	0.014288	0.016003	1030.5	2067.5	809	950	1424	2550	1687	2055
10478048	NM_00848	Lbp	2.01	0.000095	0.000204	1402.1	2813.0	1382	1268	1573	2393	3145	2958
10438784	BC086669	Gm606	-2.09	0.000729	0.001010	621.6	298.1	635	697	542	287	323	286
10571297	ENSMUST	Gm9951	-2.11	0.000001	0.000010	699.3	331.8	734	647	720	325	317	354
10600886	NM_02953	Gpr165	-2.11	0.000383	0.000589	1288.6	610.2	1597	1316	1018	714	627	508
10523506	NM_17340	Bmp3	-2.17	0.000148	0.000276	2631.4	1214.5	2694	2481	2726	1094	1308	1252
10382692	BC065414	2210020M	-2.18	0.000043	0.000125	682.7	313.6	742	707	607	317	350	278
10447860	NM_00103	Pnldc1	-2.24	0.000001	0.000010	768.9	342.9	674	804	840	327	358	344
10439321	NM_02130	Slc15a2	-2.28	0.019590	0.021595	349.5	153.1	293	460	317	207	144	120
10408543	ENSMUST	Mylk4	-2.48	0.000000	0.000007	10998.4	4438.9	11073	10860	11063	4528	4695	4115
10356154	NM_17243	Sphkap	-2.49	0.008617	0.010054	1038.1	416.5	1113	1676	600	448	525	307
10554249	NM_00742	Acan	-2.53	0.000500	0.000721	2144.5	849.0	1982	2690	1850	897	885	771